Effect of Soil Water on GPR Estimation of Bulked Roots, Methods, and Suggestions

Brody L Teare (blteare@tamu.edu)
Texas A and M University: Texas A&M University https://orcid.org/0000-0001-7122-2127
Henry Ruiz
Texas A&M University
Afolabi Agbona
Texas A&M University
Matthew Wolfe
Texas A&M University
Iliyanna Dobreva
Texas A&M University
Tyler Adams
Texas A&M University
Michael Selvaraj
Centro Internacional de agricultura Tropical CIAT: Alliance of Bioversity International and International Center for Tropical Agriculture
Dirk B Hays
Texas A&M University

Research

Keywords: Root Phenotyping, Cassava, Early storage root bulking, Ground Penetrating Radar

Posted Date: September 22nd, 2021

DOI: https://doi.org/10.21203/rs.3.rs-907807/v1

Abstract

Background: Root phenotyping methods are of increasing importance as researchers seek to understand belowground productivity and breeders work to select for root traits. Effective non-destructive root phenotyping methods do not exist for bulked-root and tuber crops such as potato and cassava. Cassava is a tropical crop widely grown by subsistence farmers throughout the tropics and is the fourth most important staple food crop in the world, yet lags in research. It has an extensive growth period sometimes exceeding 12 months. Early maturity is a major goal for breeders, but the ability to select for it is hampered by the lack of non-destructive yield estimation methods. GPR is a tool with potential to aid in bulked root selection, but standard methods have yet to be developed. In this study, we demonstrate good practice in GPR estimation of root mass, which was used as a proxy for cassava root mass, and investigate the effect of soil water content on measurement.

Results: Significant correlation between GPR data and daikon root mass was found for three of the five irrigation treatments. Correlation strength improved with increased soil water content and decreased variation of soil water content between plots. Pearson correlation coefficient varied from 0.53 – 0.79.

Conclusions: GPR can be used to estimate bulked root mass. Wet soil can improve the predictive quality of GPR data, but water content needs to be homogeneous throughout the study site and period. Determining the optimal soil water content will require further research.

Intro

Recent publications have shown the importance of plant root systems in breeding for resilience and climate change [1–4]. In addition to the importance of structural root systems, many crops are grown for their bulked roots or tubers, such as potato and cassava — two globally important crops. Cassava (*Manihot esculenta*) is a tropical plant grown for its starchy bulked roots. More than 800 million people depend on it as a staple food, and even more rely on it as an important source of starch [5]. It is commonly grown by subsistence farmers because it is hardy and harvest can be delayed until needed [6]. Cassava is the world's fourth most important basic food crop and the global harvest has increased by more than 25% since 1999, nearly doubling in some regions [7, 8]. Varieties commonly require 12 months or more before harvest maturity is reached, making early root maturity a primary factor in variety selection by farmers, and a major goal for breeders [6, 8, 9].

While many advances have been made in methods to study fibrous roots, few have been made to assist breeders of bulked root crops like cassava [3, 10–12]. Yield monitoring depends on point sampling or post-harvest metrics [13–15]. A relatively new method called shovelomics was successfully applied to cassava with some modifications, but it remains a completely destructive method with all associated disadvantages [16]. Cassava breeding is hampered by very low multiplication rates, and early trials may have only 3 clones to evaluate, making it untenable to destructively sample the roots until it is certain they have bulked [8]. This highlights the continued need for non-destructive methods to assay root crops.

In 2017, Delgado et al. reported on the use of ground penetrating radar (GPR) for estimating cassava root mass and detecting the onset of root bulking [17]. A later 2019 study by Delgado et al. furthered the work by performing high density scans on buried roots in a climate controlled sand box [18]. This study was able to approximate 3D models of the buried roots. GPR has also been used to estimate the root mass of sugar beet, wheat, and peanut [19–21]. GPR is a geophysical tool for detecting belowground features such as fault lines or buried utilities [22]. GPR works by emitting a pulse of electromagnetic energy into the ground, where it is either transmitted, absorbed, scattered, or reflected. Reflections are caused by changes in dielectric permittivity, a measure of how strongly molecules can be polarized. In agricultural soils, the primary drivers of dielectric are soil texture and water content, with water content having the greater influence by an order of magnitude. Therefore, the high water content of roots has the potential to reflect GPR signals.

In general, GPR systems consist of system electronics which generate and process the signal, a transmitting and receiving antenna or antenna array, and computer-based control and capture software. GPR data are in the time domain, and the images are not representative of spatial relations, making GPR data difficult to interpret visually. This is because the GPR is directly measuring time-of-flight for the signal, the speed of which is controlled by the dielectric of the medium, such that the velocity (V) can be estimated by the ratio of the speed of light in a vacuum (C) to the square root of the dielectric (ε) (see Eq. 1). In many cases, GPR data are used qualitatively for the location of objects rather than quantitatively [23]. Soil moisture has the effect of attenuating GPR signals; consequently, it is standard practice to prefer dry soil for GPR measurements [24]. However, in an earlier experiment which attempted to estimate fine roots with GPR, Liu et al. suggest that wet soil may improve data quality [25].

$$V = \frac{C}{\sqrt{\epsilon}}$$

Equation 1 The velocity (V) of an electromagnetic wave is dependent on the dielectric (ε) of the medium in which it travels, and is relative to the speed of light in a vacuum (C).

Delgado et al. (2017) used a small radar system which was carefully passed along the soil surface in a grid around each plant, and then measured the depth of each root to allow a supervised processing method. While this method serves as proof of concept, it is unsuitable for high-volume phenotypic evaluations common in the early-stage testing in plant breeding. GPR systems commonly use antennas which are in contact with the ground, called ground coupled. In agricultural systems, because of the soft, uneven soil, and the likelihood of standing plant mass, an air-launched antenna (antenna not ground coupled) is more appropriate. However, lifting the antenna from the ground has the potential to add observational error to the data. Air-launched antennas tend to suffer from increased ground clutter, which is the bright reflection caused by the interface of the air and soil, and any material at or near that interface, such as plant mass. Additionally, variations in the orientation of the antenna, whether caused by wobbling of the cart or other factors, can introduce variations in the measurement. Lastly, all GPR systems potentially receive interference from outside sources, such as cell phone signals or other nearby

instrumentation. These often can be minimized during the collection by stacking, which is the rapid and automatic collection and averaging of several GPR pulses.

In this paper, we describe a field ready GPR system which is more suited to high volume applications in estimating bulked root mass by using an air launched antenna array. We describe preliminary experiments in controlled field settings using a model root crop, daikon radish, and novel data processing methods for extracting quantifiable data from GPR scans. Importantly, the effect of soil water was explored. We present methods for collection, and suggest some good practices which future researchers should consider. The strength, limitations, and future potential of GPR will discussed.

Methods

Location

A raised bed of loamy sand was built in the Brazos River Bottoms, near Texas A&M University in College Station, Texas (Fig. 1). The bed is built of concrete blocks, stacked approximately 2 meters high, and the bed is approximately 3.5 by 22.5 meters long. The soil is sandy loam, transported from nearby farmland, and is kept free of weeds, therefore, the soil is homogenous and without distinct horizons. The soil was broken with a shallow till, leveled, and settled by watering before experiments began. 21 plots were measured out at 80 cm intervals, and marked off with stakes and string, then holes were carefully dug in the center of each plot. The holes were square shaped, approximately 65 cm on a side, with flat bottoms and measured 15 cm deep from the surface. The number of plots was limited by available space.

Root Mass

Daikon radish were purchased from local grocery stores then weighed and labeled individually in random order. Daikon radish were used rather than cassava because of local availability, cassava being unavailable in the required quantities. Daikon radish were considered an appropriate model root because of similarities in size and shape. The roots were placed in the holes horizontally, and arranged to maximize the angle between adjacent roots and mimic the root growth of cassava. The number of roots in each plot was varied between 1 and 5 to increase variation in plot mass and variation in root orientations (Figure 2). Enough roots were obtained to fill 19 plots. Per plot root mass ranged from 542 g to 2931 g.

Sensors

Campbell Scientific CS655 soil moisture sensors (Logan, Utah, USA) were placed in the first and last plots, at two depths: 5 cm and 20 cm. The sensors were inserted horizontally into the undisturbed soil on the side of the plots. Moisture levels were recorded before radar scanning. Additionally, 2 flat metal plates were place in the first and second plot at the same depths as the sensors, so that the plates straddled the root zone. These were meant to demarcate the root zone in the GPR data by acting as distinct reflectors.

The radar sensor used was an experimental loaded-vee dipole array, manufactured by IDS Georadar (Pisa, Italy) [26–28]. The array consists of 4 transmitters and 4 receivers in alternating pairs, each spaced 4 cm from adjacent antennas (Fig.3). The antennas are wideband with a center frequency of 1.8 GHz. The radar captures 512 samples over 18 ns, and pulses every 1 cm, as measured by an encoder wheel. Channel configurations paired every antenna with its directly adjacent neighbor, giving a total of 7 channels, each offset by 4 cm. The sampling time increases with the number of channels, and in this case prevented automatic stacking as that would result in lost data due to hardware limitations of sampling speed.

The array was air launched, and mounted on a 4 wheeled cart that straddled the plots and placed the bottom of the antenna enclosure 39 cm from the ground surface (Fig. 4). The antenna was pointed directly at the ground, and a plastic rod was attached at the center of the enclosure to give a ground indication of the nadir of the radar. The plastic rod indicated the center of the antenna at ground level, and was used as a reference for marking the plots digitally in the capture software.

Soil Moisture

The experiment was scanned at 5 different water contents, beginning with a ‘dry’ state. Two oscillating sprinklers were placed in the field such that the sprays evenly covered the entire expanse without overlap. The sprinklers were measured to provide about 13.5mm per hour by collecting water in two 5-gallon buckets placed in the sprinklers’ path. The sprinklers were run for times varying from 2 hours to 8 hours, then the field was allowed to rest between 4 and 48 hours before scanning, allowing surface pools to drain and attempting to let subsurface moisture equalize spatially. Table 1 shows the percent volumetric water content (VWC) of each treatment, and the standard deviation across the sensors.

Table 1
Average volumetric water content of each treatment, and the standard deviation as percent water, volume/volume basis.

	No Irrigation	Irrigation 1	Irrigation 2	Irrigation 3	Irrigation 4
Average VWC	12.5%	17.3%	16.7%	18.6%	16.7%
Standard Dev.	0.86%	3.68%	3.24%	3.11%	1.7%

Capture

The GPR cart was assembled in the field and given time to equilibrate to ambient temperatures. Before collecting data, several scans were passed across the entire transect to allow the electronics to “warm up”. More than 1 meter was allowed between the starting position of the cart and the first plot, and the ending position and the last plot, to ensure the radar captured the entire extent. Using the plastic rod (Fig. 4e) and string as an indicator, a digital marker (fiducial) was placed in the data in between each plot. The experiment was scanned 6 times for each treatment.

Data Processing and Analysis

Data was processed using GPR Studio version 1.0 (Crop Phenomics LLC, College Station, TX, USA), a Python software library developed for the quantitative analysis of GPR data. The software utilizes published data processing libraries and custom-built functions specific to GPR analysis. Analysis was conducted in two stages.

In Stage 1, each scan was separated into plots based on the digital markers placed in the data during field capture. The plots were then filtered to only those containing roots. Data were subset to the approximate root zone, then passed through a Butterworth bandpass filter, removing noise below 0.5 GHz and above 1.05 GHz. The 7 channels were each standardized to themselves by subtracting the channel mean from each value, and dividing by the channel standard deviation, similar to how a statistical z-score is calculated. This removed offset differences between channels caused by automated signal calibration in the field. Standardized channels were then squared to move all values to the positive domain and minimize the background information which tends to gather about the mean, or 0 in standardized data. Channels were interpolated into a 3D cube using linear interpolation. A horizontal window, or time slice, 5 rows deep was passed from the top of the cube to the bottom, summing the amplitude in each window, which can be considered an indicator of total reflected energy in that window. Several window depths and alternative measurements, such as window variance, were tested – the most effective is reported here. Window values were correlated against known root mass in each plot, the results filtered for p-value < 0.1, while also controlling for appropriateness in the depth of the window and consistency between observations. The depth with the lowest p-value was stored for further processing. The cumulative energy values for each plot were divided by the length of that plot, in scan columns, resulting in relative energy density (Fig. 5).

In Stage 2, the results of Stage 1 for repeated observations were averaged together to reduce observational variance. Table 1 shows the mean energy density per plot with the standard error of the mean (SEM), and the coefficient of variation (CV) for each plot and treatment, demonstrating the observational variance in each repeated scan. Observational variance is an indication of noise in the data, which is a significant source of error here, and is further discussed below. Repeated observations help to remove the error through averaging.

Linear regression analysis was performed between the averaged energy density and the known root mass.

Table 2

Observational variance per plot, the mean relative energy density for each plot and treatment, and the coefficient of variation. Plots are arranged in order of increasing root mass to aid interpretation.

	Dry		Irrigation 1		Irrigation 2		Irrigation 3		Irrigation 4	
	Mean	C.V.	Mean	C.V.	Mean	C.V.	Mean	C.V.	Mean	C.V.
Plot 1	7.03 ± 0.31	10.7%	6.77 ± 0.87	31.5%	6.96 ± 0.68	19.6%	4.89 ± 0.19	7.6%	4.71 ± 0.42	19.8%
Plot 2	6.71 ± 0.51	18.5%	8.17 ± 1.25	37.6%	6.87 ± 0.35	10.1%	5.91 ± 0.7	23.7%	5.46 ± 0.75	30.5%
Plot 3	6.31 ± 0.43	16.7%	4.86 ± 0.34	17.1%	6.73 ± 0.54	16.0%	7.18 ± 1.87	52.0%	6.85 ± 0.7	22.8%
Plot 4	7.11 ± 0.29	9.8%	8.21 ± 0.86	25.6%	8.75 ± 0.84	19.3%	8.14 ± 1.53	37.5%	6.44 ± 1.05	36.3%
Plot 5	7.68 ± 0.36	11.4%	6.26 ± 0.52	20.3%	8.81 ± 0.72	16.3%	7.14 ± 0.4	11.3%	6.48 ± 0.76	26.2%
Plot 6	5.39 ± 0.42	19.1%	4.79 ± 0.4	20.5%	7.98 ± 0.85	21.3%	6.93 ± 2.26	65.3%	5.91 ± 1.02	38.7%
Plot 7	6.02 ± 0.38	15.3%	6.29 ± 0.8	31.3%	7.58 ± 0.82	21.5%	5.90 ± 0.64	21.9%	6.06 ± 0.88	32.4%
Plot 8	8.04 ± 0.23	7.1%	6.17 ± 0.88	34.8%	7.30 ± 0.42	11.4%	5.57 ± 1.09	39.2%	5.85 ± 0.76	29.0%
Plot 9	6.00 ± 0.31	12.8%	5.96 ± 0.62	25.5%	6.82 ± 0.84	24.6%	6.01 ± 0.99	33.1%	5.85 ± 0.97	37.1%
Plot 10	8.22 ± 0.42	12.5%	7.43 ± 0.89	29.4%	8.73 ± 0.51	11.8%	7.44 ± 0.36	9.7%	8.15 ± 1.29	35.5%
Plot 11	7.95 ± 0.22	6.8%	8.92 ± 1.2	32.8%	7.73 ± 0.61	15.8%	6.08 ± 0.42	13.9%	7.05 ± 0.86	27.4%
Plot 12	7.03 ± 0.30	10.3%	7.68 ± 0.79	25.1%	8.70 ± 0.33	7.7%	6.30 ± 0.57	18.1%	5.90 ± 0.76	28.7%
Plot 13	8.23 ± 0.36	10.6%	7.29 ± 0.97	32.7%	7.34 ± 1.17	31.9%	6.79 ± 1.05	30.8%	7.42 ± 0.98	29.4%
Plot 14	8.49 ± 0.45	13.0%	8.84 ± 1.05	29.2%	9.88 ± 0.48	9.8%	8.13 ± 0.5	12.3%	8.60 ± 1.22	31.7%
Plot 15	7.33 ± 0.32	10.6%	6.40 ± 0.56	21.6%	10.12 ± 0.86	17.0%	7.43 ± 1.72	46.2%	10.11 ± 0.97	21.5%
Plot 16	8.42 ± 0.40	11.5%	8.90 ± 1.6	44.1%	6.05 ± 0.31	10.2%	6.70 ± 1.25	37.4%	5.90 ± 0.62	23.4%
Plot 17	7.90 ± 0.45	14.0%	6.89 ± 0.64	22.9%	9.80 ± 1.11	22.6%	6.91 ± 1.17	33.9%	8.87 ± 0.76	19.1%

	Dry		Irrigation 1		Irrigation 2		Irrigation 3		Irrigation 4	
Plot 18	8.69 ± 0.37	10.4%	11.11 ± 1.36	30.0%	10.34 ± 0.72	13.9%	9.61 ± 1.21	25.2%	10.51 ± 1.55	33.1%
Plot 19	8.44 ± 0.33	9.6%	8.26 ± 0.97	28.9%	9.32 ± 0.77	16.6%	10.07 ± 1.56	30.9%	10.22 ± 1.4	30.7%

The metal plates placed above and below the root zone were not identifiable in the radar data, possibly because of the type of paint applied to them. Therefore, it was not possible to use them to fine tune the root zone as had been planned.

Results

Our results demonstrate a significant relationship between reflected GPR signal and bulked root biomass. Additionally, the results demonstrate the importance of a homogenous dielectric environment in the soil, independent of water content. Lastly, we show that for relatively shallow agricultural studies, dry soil is not necessarily superior to wet soil for GPR measurement, a finding which supports the hypothesis of Liu et al, 2018 [20].

All treatments were significant at the $p < 0.05$ level. The final treatment, which had the most homogenous wet soil but not the wettest, showed the strongest correlation, followed by the wettest treatment, then the dry treatment, which had the least variation in soil moisture. Larger variation in soil moisture decreased the strength of the correlations (Fig. 6). Although the number of plots was low, the repeated measurements and multiple treatments reinforces the probability that GPR features are indicative of root mass, and are not random. Dividing the sum of energy by the scan length modestly improved the correlations by adjusting for the effect of scan length, indicating that scan length was not a significant contributor to the correlations, but that variations in scan length introduced error.

The window depth of significant correlations varied slightly between treatments, which is expected as an effect of the varying dielectric. The depth of the dry treatment was greater than the wet treatments, which is unexpected, and will be discussed below. Standard deviation of the plot size, as measured by scan lengths, was 2.86 cm, less than 4% of the target plot length of 80 cm, and was randomly distributed in relation to plot number, observation, and treatment. Standard deviation between observations, within treatments, was not correlated to volumetric water content (VWC), variation of VWC, or plot biomass. The only exception for this is the Irrigation 4 treatment, in which relative energy density deviation was correlated to plot biomass at the $p < 0.05$ level.

Table 2
Summary of the mean relative energy density of each treatment and the regression results.

Treatment	Mean Energy	Energy σ	Depth	Pearson r	r2	Slope	Intercept	p-value
No Irrigation	7.422	0.954	66	0.645	0.415	458.7	-1901.7	0.0029
Irrigation 1	7.326	1.513	40	0.530	0.281	238.1	-241.6	0.0195
Irrigation 2	8.201	1.262	45	0.564	0.318	303.3	-984.9	0.0119
Irrigation 3	7.007	1.270	40	0.653	0.426	349.2	-944.1	0.0024
Irrigation 4	7.176	1.698	48	0.792	0.626	316.6	-769.3	0.000054

Discussion

Rapid estimation of bulked root mass is possible with GPR. These results show correlation strength up to 79% using these methods. Further, we have demonstrated that increased VWC can improve the detection of bulked roots, as long as the dielectric is homogeneous across the study. The bulk dielectric of soil is driven primarily by water, and the interfaces of dielectric change cause the reflection of GPR energy. With a sufficiently high signal frequency, soil structure has the potential to introduce noise in GPR data through the minute reflection and scattering of EM energy, driven by soil features such as compaction layers, aggregates, and pores. By increasing the VWC, some soil pores fill with water, and the dielectric heterogeneities are reduced, leading to less noisy GPR data. Additionally, as the dielectric of the soil increases, the signal velocity reduces, effectively increasing the sampling resolution of the system, as the sampling is a function of time.

These two factors may explain why increased VWC improved the strength of correlation. Indeed, we hypothesize that as VWC variance decreases, the strength of the correlation should increase, possibly maximizing the predictive potential near field capacity. Unfortunately, soils near field capacity are easily compacted, and are difficult to work in. Therefore, some compromise must be found to maximize predictive power of the GPR and minimize the impact and difficulty of field work. This optimal level of soil moisture is most likely dependent on soil texture, and could be expressed as a fraction of field capacity. Further studies in multiple soil types should lead to standardized recommendations of optimum water content for major texture groups.

This study, like others before it, presents a supervised correlation – that is, the depth and mass of roots is known, so it becomes less difficult to determine the optimum depth of radar information to analyze. The window of analysis is relatively narrow – only five rows, or approximately 2 cm of soil depth – and selecting the correct depth without previous knowledge of the root depth is difficult at this time. As research continues, it may become possible to distinguish the zone of highest information density, and researchers are already working towards that goal [21]. In this study, however, the noise was too great to establish the root zone from only GPR data. For this application, noise may be considered as all recorded

energy which is not reflected by plant roots. As discussed earlier, GPR systems record all intercepted energy in the antenna range, regardless of the energy source. Noise may also be generated within the GPR system itself, and there has been some indication that the prototype system used here is not immune to this type of noise. This can be reduced by careful engineering, and through data filtering, if the inherent noise has been characterized. Other sources of noise include reflections and scattering caused by variations in soil structure, stones, clay clods, surface roughness, and above-ground biomass. Because we placed roots in the soil, rather than growing them, aboveground biomass was not an issue in this study, but has been in other data which are not yet published.

As noted, the soil type and water content have a large effect on GPR data. This variation makes it difficult to build a unified correlation between studies, fields, or even dates. As such, GPR remains a relative measure of root mass, suitable for ranking within a single field and date, otherwise requiring a specific calibration at each use. It remains possible that a correction factor could change this. Inclusion of multiple blank plots in the study may provide that correction factor, such that data can be normalized to the feature values of the blank plot, accounting for the soil type and moisture content. Further studies are planned to investigate this possibility. Without locational correction, GPR data may still be used to rank plots for genotype, and rankings may be compared across locations and/or time.

These results demonstrate the effect of soil moisture not just on the ability to pick out roots, but also the effect on the method. As mentioned in the results, the depth of best correlation was deeper for the dry treatment than the irrigated treatments, which was unexpected. GPR energy is reflected at the interface of dielectric contrast. When the object causing the reflection, such as a root, has sufficient diameter, the reflection may happen at both interfaces on the signal vector – that is, it can reflect from both the top and bottom of the root. In other uses of GPR, the thickness of large objects can be estimated by measuring the distance between the top and bottom reflection. In this study, however, discreet returns were not observed; rather, the total reflected energy for a volume was measured. It is possible the reflected energy in the dry treatment was more intense at the bottom of the root, whereas the irrigated treatments reflected primarily from the upper interface. In all treatments, a nearly continuous range of window depths showed significant correlation to root mass, indicating that information about the root mass was present across a depth corresponding approximately to the root diameters. This also suggests the possibility of some distinct characteristic for that region, such that it may be possible to find that region using machine learning techniques, so that supervised correlation is no longer required, and furthering the usefulness of GPR as a predictive tool.

In 2019, Delgado et al. reported a similar study designed to test commercially available GPR models in bulked root imaging [18]. A C-Thrue GPR system (IDS Georadar) was mounted to a computer controlled gantry and passed over a climate controlled sandbox. Cassava roots of varying sizes were buried at orientations parallel, orthogonal, and 45° to the scan direction. A single antenna pair was passed in transects at 2.5 cm intervals over the sandbox, with signal pulses every 0.2 cm. The GPR data were interpolated to form 3D models of the buried roots and interpolated image dimensions were compared to physical dimensions. The study illuminates several important factors for the application of GPR to root

measurement, namely, the superiority of vertical antenna polarization over horizontal, and the effect of root orientation on measurement accuracy. However, the study differs significantly from the current – the focus was on 3D imaging rather than mass estimation, a single antenna pair was used in a high-density grid rather than an antenna array, the antenna was ground coupled rather than air-launched, and the soil medium was air dry such that no effect of soil water content was studied. Finally, the data collection method was not appropriate for high volume phenotyping.

The application of GPR for the quantification of roots is still in its infancy, and significant research is required before it can be used as a predictive tool. We have shown here that GPR data contain information about root mass, but it is also clear that other factors influence the data, and noise is a problem. Radar data is highly sensitive to processing parameters, such that adding or removing a step readily effects correlation. The presented methods utilized a multi-channel radar to rapidly collect 3D information. To produce the 3D information, the channels were interpolated using simple linear interpolation. Similar to other 3D data, such as LiDAR, care must be taken to align the interpolated entities. In the case of GPR, the primary point of alignment is usually the soil surface, because it is discrete and constant. In this study, the field was level, and the antenna was facing straight down at nadir, resulting in well-aligned channels with consistent positioning of the surface between channels. This is not always possible. In many cases, the antenna array cannot pass directly over the center of the root mass because plants are still present, so the antenna may be angled to point towards the plant center. Additionally, errors in channel calibration can produce small offsets that change the apparent height of the antenna relative to the ground surface. Finally, uneven ground surface can cause differences between channels. In these cases, the ground surface must be identified in each channel so they can be aligned before interpolation, as described by Dobreva et al [21]. Automated methods of identifying the ground surface would greatly reduce the time required for channel alignment.

Though each application will have its unique problems, there remain several constant considerations which we suggest become standard practice when using GPR to measure roots. Foremost among these is to understand your radar system. Unlike visual tools such as LiDAR, GPR emissions are not highly focused and are generally shaped like an ellipsoid bubble, meaning the energy extends in front of, behind, and to the sides of the antenna. This is why at least 1 m was allowed between the cart and the first study plot, so that initial readings would be outside the plot. This also means care must be taken for transitory reflectors, such as workers, to not enter the volume of sensitivity while collecting the data.

GPR data are highly dependent on the dielectric of the soil; therefore, it is strongly recommended that dielectric measurements always be made at the time of scanning. This can be done in many ways, such as measuring dielectric directly with a probe, measuring water content and converting using the Topp equation, or by burying a reflector at a known depth, which allows a velocity estimation by dividing the known depth below the surface by the difference in signal time from the surface to the reflector [24, 29]. Knowing the dielectric, or the signal velocity (see Eq. 1), allows the conversion of data from the time domain to the space domain, enabling estimation of depth. Further, some GPR processing techniques

require these parameters. Many studies will be interested in the root mass at certain depths, as is currently measured with destructive techniques. This is only possible if the signal velocity is known.

Published methods to date have relied on measuring reflected energy, whether by amplitude threshold and pixel counting, or summations of other features. These techniques are inherently tied to the volume of soil analyzed, meaning that plot size will auto-correlate with feature count. Plot size must therefore be carefully controlled. In this study, plot size was controlled in the field through careful measurement and marking. Other studies have controlled plot size by cropping the data, and others have controlled by conversion to either feature density, root density, or both. We recommend the former whenever possible, as it protects the integrity of the data. However, current root phenotyping methods frequently use root density as a measurement and is acceptable to many researchers [30].

Whichever way the plot length is controlled, the data must be related to the field. Some GPR systems are capable of integrating GPS data into the scan data, while others can utilize digital markers. Some have neither capability, thus plot positions must be derived another way, possibly by placing reflectors at plot ends. Experience dictates caution in the latter method – the reflector must be easily identifiable in the radargram, and reflectors placed on the soil surface are easily lost in the surface reflection. In such cases, an aerial reflector is recommended.

Finally, based on the results of this study, care must be taken to ensure homogeneous dielectric environment at the time of scanning. Depending on the hydraulic conductivity of the soil, several days may be required after an irrigation event.

Conclusion

The use of GPR technology to quantify root mass in agricultural fields is still very young and is yet to be widely accepted. However, interest is growing as more studies are published showing the potential. With up to 63% explained variability ($r^2 = 0.626$, $r = 0.792$), this study confirms previous publications, and demonstrates the feasibility of an air-launched antenna array for rapidly collecting GPR-based root estimations. Further, it is the first study to show improved data quality for wet soil over dry soil. It is novel in demonstrating the importance of dielectric homogeneity for estimating root mass. Though this study was small and should be confirmed with more samples, it serves as a proof of concept that merits further investigation. Importantly, we have demonstrated considerations in the use of agricultural GPR and begun the work of establishing a standardized method.

Abbreviations

GPR
Ground Penetrating Radar
VWC
Volumetric Water Content

V
Signal Velocity
C
Speed of light in a vacuum ≈ 0.3 m/ns

Declarations

Ethics Approval – Not applicable

Consent for Publication – Not applicable

Availability of Data and Materials – The datasets used and/or analyzed during the current study are available from the corresponding author on reasonable request.

Competing Interests - The authors declare that they have no competing interests

Funding – This work was supported with grants from the National Science Foundation award number 1543957—BREAD PHENO: High Throughput Phenotyping Early Stage Root Bulking in Cassava using Ground Penetrating Radar to Dirk B. Hays, and by the Department of Energy of the United States (ARPA-E Award, No. DE-AR0000662)—Development of ground penetrating radar for enhanced root phenotyping and carbon sequestration also to Dirk B. Hays.

BT performed the data acquisition, data processing and analysis, and wrote the manuscript. HR assisted with acquisition and created the software framework used in data processing. AA assisted with statistical analysis. MW assisted with data acquisition and interpretation. ID assisted in creating the software. TA provided substantial assistance in revising the manuscript. DH aided with conception, design, and data acquisition.

Acknowledgments – Not applicable

References

1. Lal R (2004) Soil carbon sequestration to mitigate climate change. Geoderma 123:1–22
2. Lynch JP (2007) Roots of the Second Green Revolution. Aust J Bot 55:493
3. Atkinson JA, Pound MP, Bennett MJ, Wells DM (2019) Uncovering the hidden half of plants using new advances in root phenotyping. Curr Opin Biotechnol 55:1–8
4. Lynch JP (2013) Steep, cheap and deep: an ideotype to optimize water and N acquisition by maize root systems. Ann Bot 112:347–357
5. Nassar N, Ortiz R (2010) Breeding Cassava to Feed the Poor. Sci Am 302:78–84
6. Okechukwu RU, Dixon AGOO (2009) Performance of Improved Cassava Genotypes for Early Bulking, Disease Resistance, and Culinary Qualities in an Inland Valley Ecosystem. Agron J 101:1258–1265

7. Ceballos H, Hershey C, Becerra-López-Lavalle LA (2012) New Approaches to Cassava Breeding. In: Plant Breed. Rev. John Wiley & Sons, Inc., Hoboken, NJ, USA, pp 427–504
8. Ceballos H, Iglesias CA, Pérez JC, Dixon AGO (2004) Cassava breeding: opportunities and challenges. Plant Mol Biol 56:503–516
9. Kamau J, Melis R, Laing M, et al (2011) Farmers ' participatory selection for early bulking cassava genotypes in semi-arid Eastern Kenya. J Agron Crop Sci. https://doi.org/10.5897/JPBCS.9000053
10. Maeght J-L, Rewald B, Pierret A (2013) How to study deep roots—and why it matters. Front Plant Sci 4:299
11. Kuijken RCP, Van Eeuwijk FA, Marcelis LFM, Bouwmeester HJ (2015) Root phenotyping: From component trait in the lab to breeding. J Exp Bot 66:5389–5401
12. Paez-Garcia A, Motes C, Scheible W-R, Chen R, Blancaflor E, Monteros M (2015) Root Traits and Phenotyping Strategies for Plant Improvement. Plants 4:334–355
13. Durrence JS, Perry CD, Vellidis G, Thomas DL, Kvien CK (2015) Mapping Peanut Yield Variability with an Experimental Load Cell Yield Monitoring System. 1131–1140
14. Malay WJ, Gordon RJ, Madani A, Patterson GT, Esau C, Eaton LJ, LeBlanc P (2000) Root Crop Yield Monitor Evaluation for Carrots. In: 2000 ASAE Annu. Intenational Meet. Tech. Pap. Eng. Solut. a New Century. American Society of Agricultural Engineers, pp 3039–3050
15. Davenport JR, Redulla CA, Hattendorf MJ, Evans RG, Boydston RA (2002) Potato Yield Monitoring on Commercial Fields. Horttechnology 12:289–296
16. Kengkanna J, Jakaew P, Amawan S, Busener N, Bucksch A, Saengwilai P (2019) Phenotypic variation of cassava root traits and their responses to drought. Appl Plant Sci 7:e01238
17. Delgado A, Hays DB, Bruton RK, Ceballos H, Novo A, Boi E, Selvaraj MG (2017) Ground penetrating radar: a case study for estimating root bulking rate in cassava (Manihot esculenta Crantz). Plant Methods 13:65
18. Delgado A, Novo A, Hays DB (2019) Data Acquisition Methodologies Utilizing Ground Penetrating Radar for Cassava (Manihot esculenta Crantz) Root Architecture. Geosciences 9:171
19. Miodrag Konstantinovic, Sebastian Woeckel, Peter Schulze Lammers, Juergen Sachs, Konstantinovic M, Woeckel S, Lammers PS, Sachs J (2007) Evaluation of a UWB radar system for yield mapping of sugar beet. Am Soc Agric Biol Eng Meet Present 71051:1–11
20. Liu X, Dong X, Leskovar DI, Xue Q, Marek T, Jifon J, Butnor JR (2018) Ground penetrating radar (GPR) detects fine roots of agricultural crops in the field. Plant Soil 517–531
21. Dobreva ID, Ruiz-Guzman HA, Barrios-Perez I, Adams T, Teare BL, Payton P, Everett ME, Burow MD, Hays DB (2021) Thresholding Analysis and Feature Extraction from 3D Ground Penetrating Radar Data for Noninvasive Assessment of Peanut Yield. Remote Sens 13:1896
22. Everett ME (2013) Near-Surface Applied Geophysics. Near-Surface Appl Geophys. https://doi.org/10.1017/CBO9781139088435

23. Baker GS, Jordan TE, Pardy J (2007) An introduction to ground penetrating radar (GPR). In: Spec. Pap. 432 Stratigr. Anal. Using GPR. Geological Society of America, pp 1–18
24. Utsi EC (2017) Ground Penetrating Radar : Theory and Practice. Elsevier Science, Oxford, UK
25. Liu X, Dong X, Xue Q, Leskovar DI, Jifon J, Butnor JR, Marek T (2018) Ground penetrating radar (GPR) detects fine roots of agricultural crops in the field. Plant Soil 423:517–531
26. Nuzzo L, Alli G, Guidi R, Cortesi N, Sarri A, Manacorda G (2014) A new densely-sampled Ground Penetrating Radar array for landmine detection. In: Proc. 15th Int. Conf. Gr. Penetrating Radar. IEEE, pp 969–974
27. Montoya TP, Smith GS (1996) Vee dipoles with resistive loading for short-pulse ground-penetrating radar. Microw Opt Technol Lett 13:132–137
28. Kangwook Kim, Scott WR (2005) Design of a resistively loaded vee dipole for ultrawide-band ground-penetrating Radar applications. IEEE Trans Antennas Propag 53:2525–2532
29. Topp GC, Davis JL, Annan AP (1980) Electromagnetic determination of soil water content: Measurements in coaxial transmission lines. Water Resour Res 16:574–582
30. Smit AL, Bengough AG, Engels C, van Noordwijk M, Pellerin S, van de Geijn SC (2000) Root Methods. https://doi.org/10.1007/978-3-662-04188-8

Figures

Figure 1. Study was conducted in large raised beds filled with sandy loam soil. Plots were carefully measured and marked by string.

Figure 1

Study was conducted in large raised beds filled with sandy loam soil. Plots were carefully measured and marked by string.

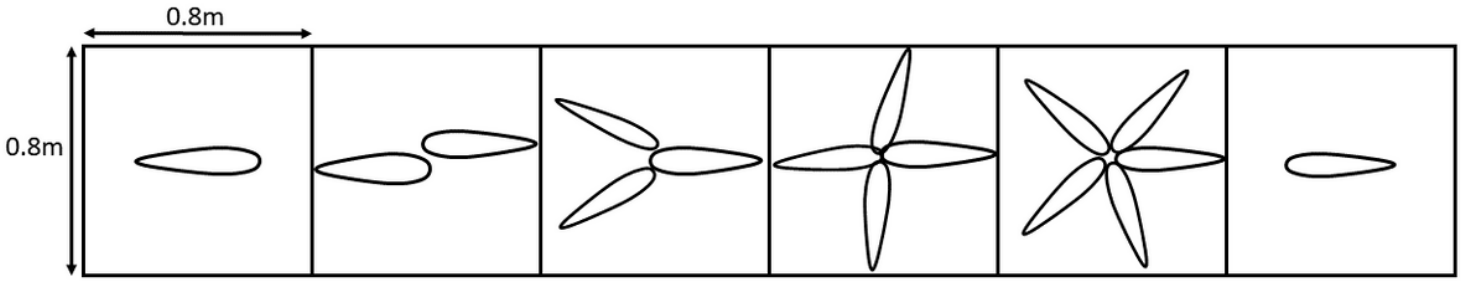

Figure 2

Roots were placed horizontally to maximize the angle between adjacent roots, as space allowed. Plots contained between 1 and 5 roots.

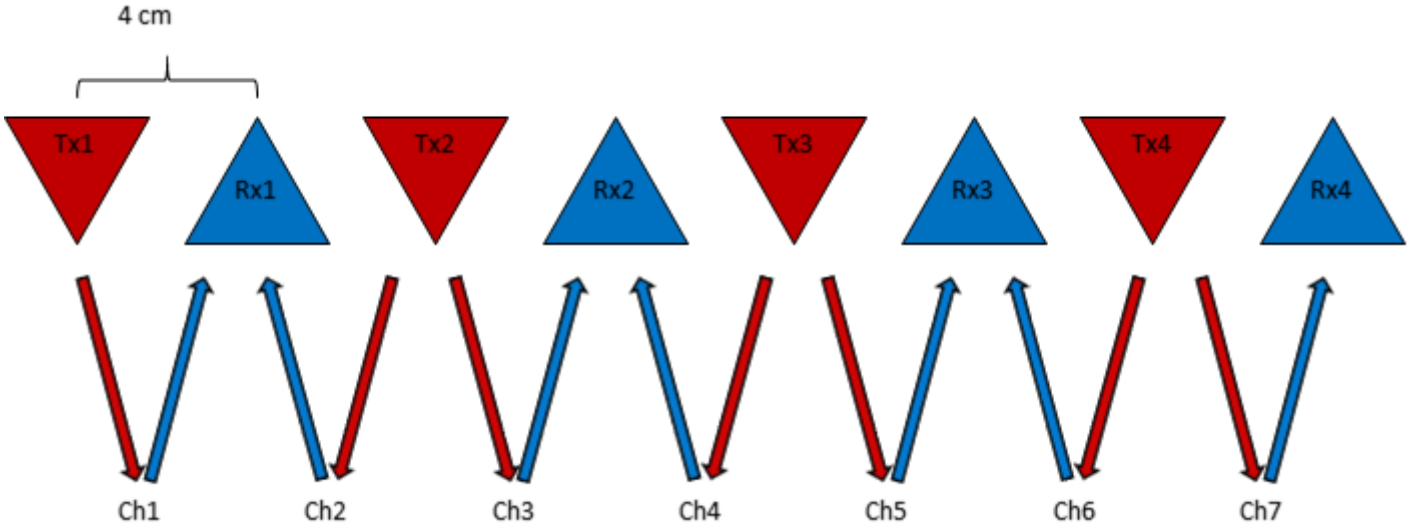

Figure 3

The antenna array consisted of 4 transmit and 4 receive antennas, spaced evenly 4 cm apart. 7 scan channels paired each antenna with its neighbors. Tx designates a transmitting antenna, while Rx designates a receiving antenna, Ch indicates a channel pairing.

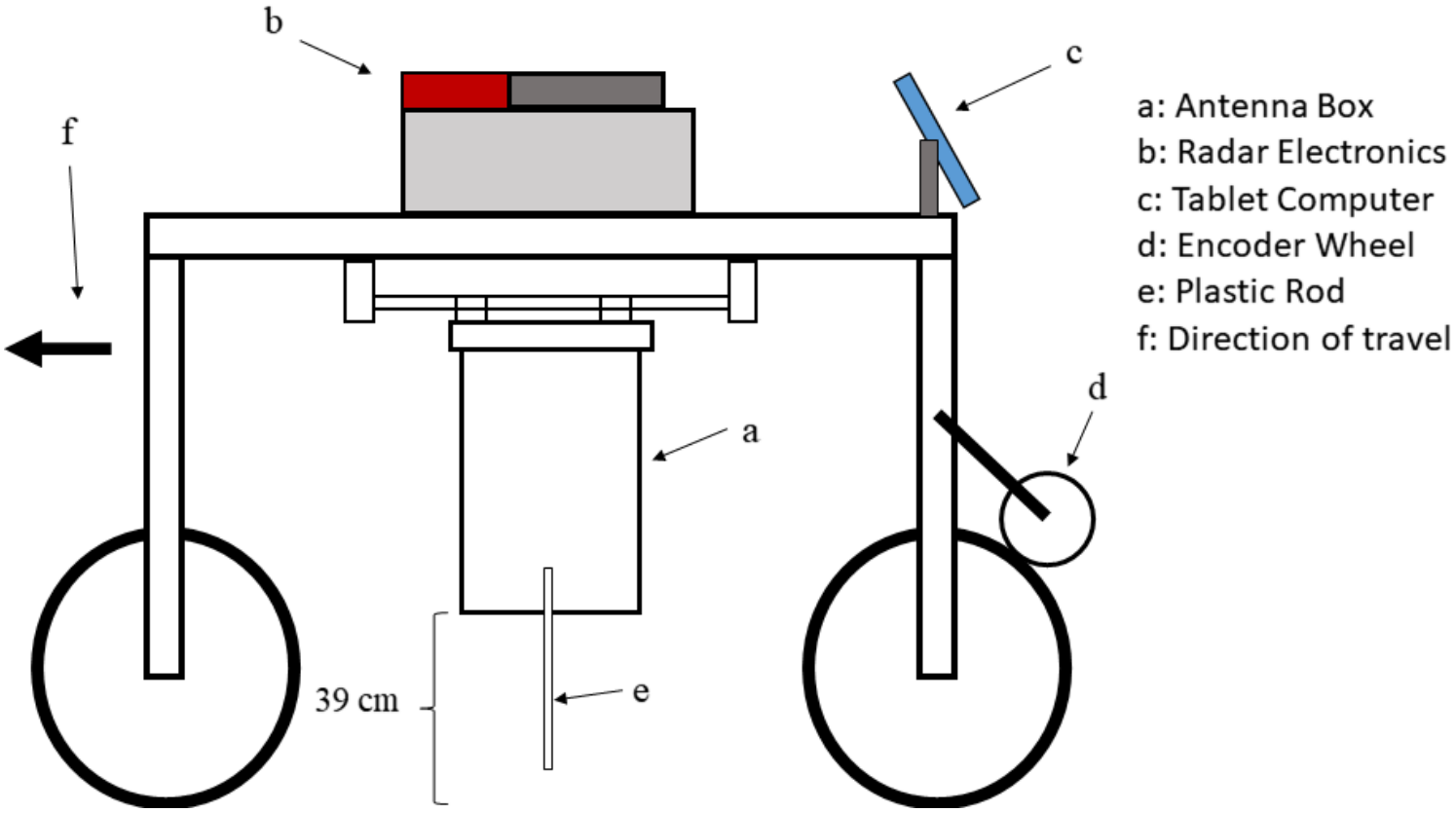

Figure 4

The antenna cart had 4 wheels and straddled the plots. The antenna array was hung in the middle with a plastic rod on one side to indicate the position of the center of the array on the ground.

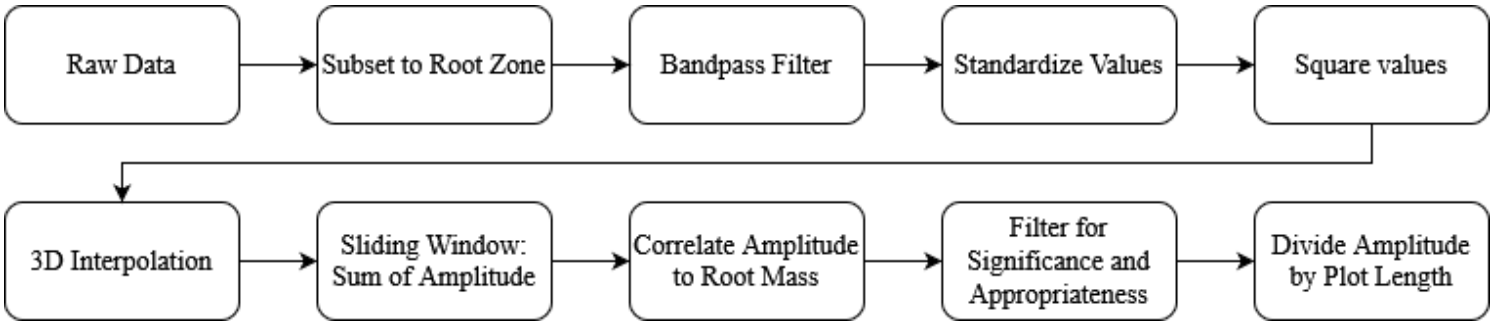

Figure 5

Stage 1 of the data processing workflow.

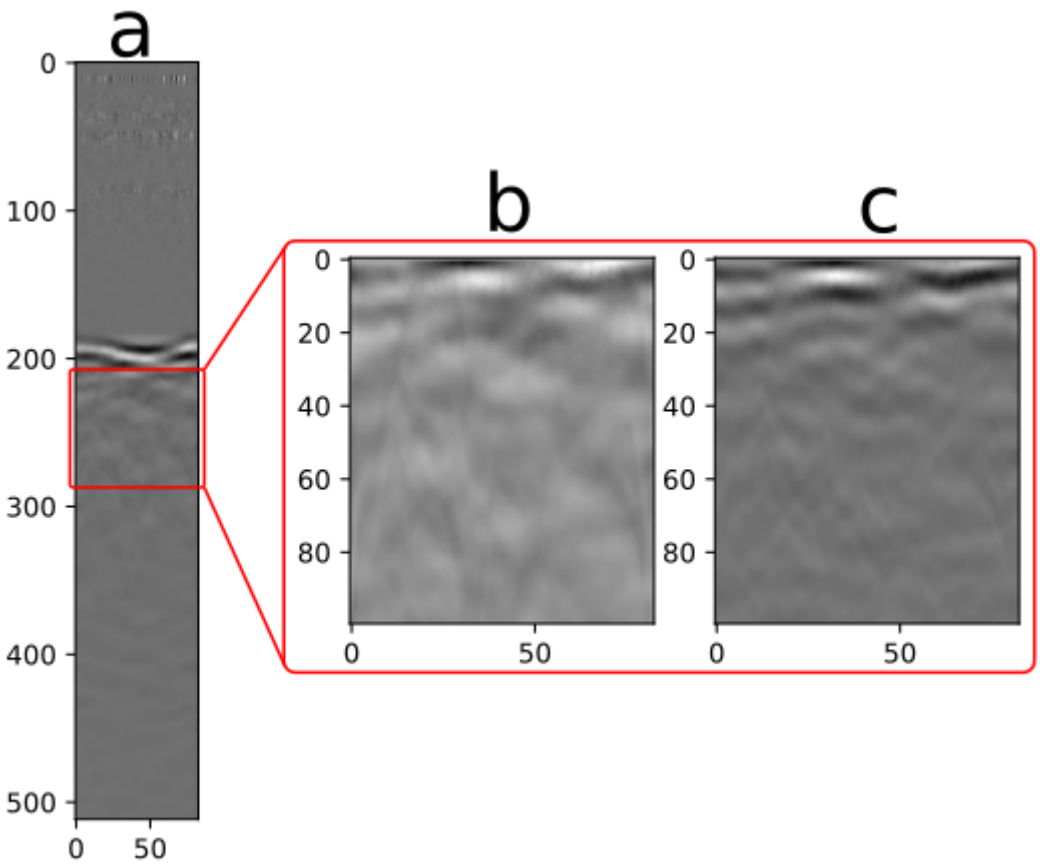

Figure 6

Sample radargrams from Stage 1 of the processing workflow. In unprocessed GPR data, both white and black represent high amplitude energy reflections, albeit at opposite phase angles. Low energy is shown as grey. A - Raw data showing a single plot. Notice the surface reflection near line 200. B- Plot cropped to the root zone, corresponds to lines 205 to 305 on left image. C - Standardized plot.

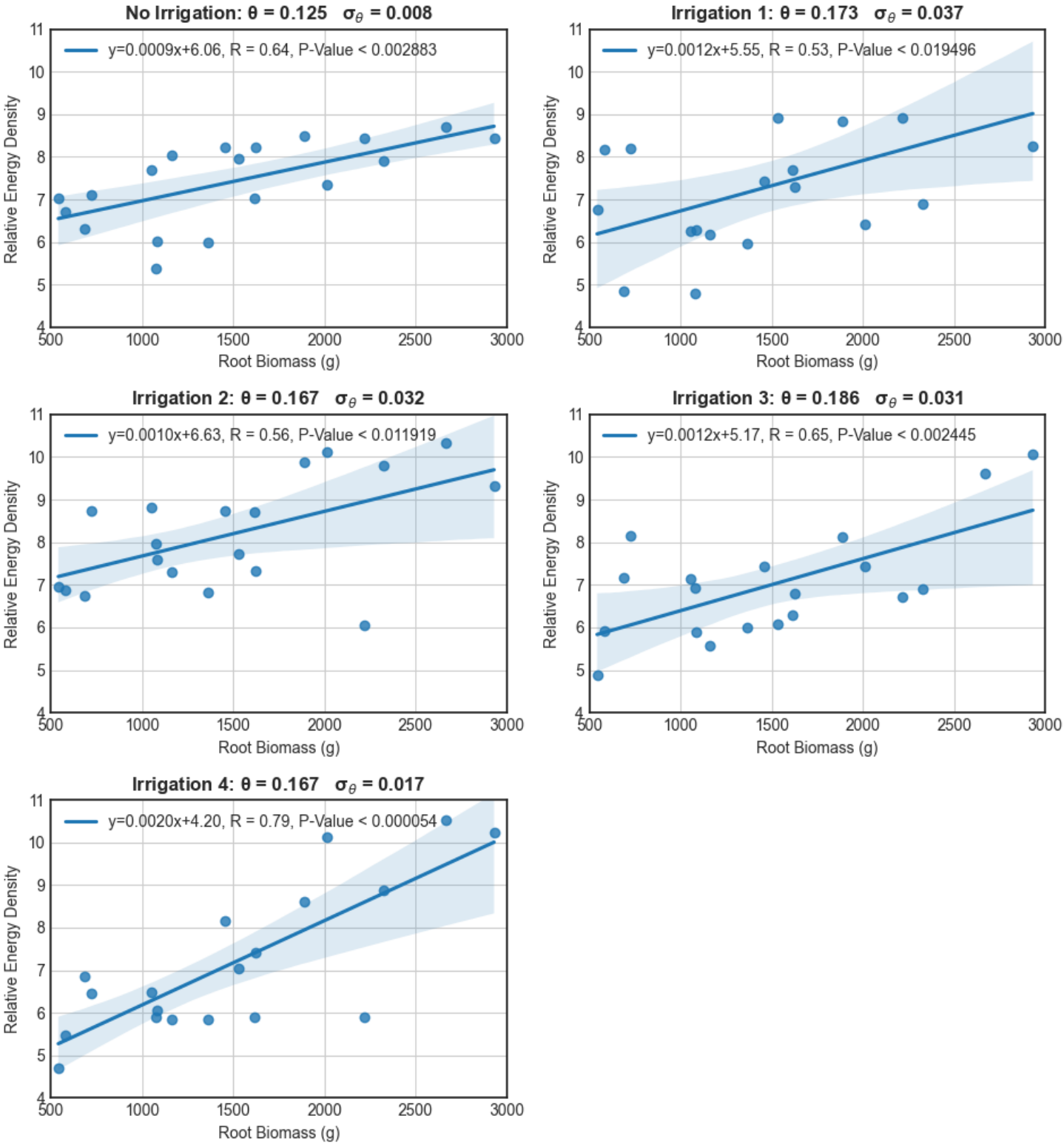

Figure 7

Correlation regression for all 5 treatments. Shaded area indicates 95% confidence interval based on 10,000 iterations of bootstrap testing. Note that Θ represents VWC. While the un-irrigated treatment had the lowest variation in VWC, the Irrigation 4 treatment had the strongest correlation, indicating the potential reduction of noise in wet soils vs dry soil. Irrigation 1 had the highest VWC variance, and the weakest correlation.